Special Issue

Institution of MECHANICAL ENGINEERS
Journal of MATERIALS: DESIGN AND APPLICATIONS

Proc IMechE Part L:
J Materials: Design and Applications
0(0) 1–9

DOI: 10.1177/1464420715571189
pil.sagepub.com
SAGE

Friction stir processing of Al–CNT composites

Zhenglin Du[1], Ming-Jen Tan[1], Jun-Feng Guo[2] and Jun Wei[2]

Abstract

Friction stir processing (FSP) is a solid-state process with the ability to refine grain sizes and uniformly disperse particles to improve the mechanical properties of the base material. In this study, FSP was performed on AA6061-T6 with and without additions of multi-walled CNTs. For FSP on monolithic Al plates, dendrites were broken down and dispersed uniformly with the increase in number of passes. As for FSP of Al–CNT composites, the CNTs have been successfully dispersed with three FSP passes. Dispersion is more uniform with increasing number of passes. The Vickers hardness and tensile yield strength were found to have improved after performing FSP with the addition of CNT as compared to FSP of AA6061-T6 without CNT.

Keywords

Friction stir processing, nanocomposites, carbon nanotubes, mechanical properties

Date received: 28 August 2014; accepted: 18 December 2014

Introduction

Friction stir welding and friction stir processing

Friction stir welding (FSW) was invented by The Welding Institute (TWI) of UK in 1991.[1] It is a solid-state joining technique used to weld two pieces of metal together without melting. Much research has been done on the welding of aluminum due to its relative low melting pointing and low weldability using traditional welding techniques.

The basic working principle of FSW involves a nonconsumable tool with a threaded pin and shoulder being plunged into the abutting edge of two sheets and transverse along the direction of the line of joint. The friction between the tool and the plate generates heat which softens the work piece. The rotation of the tool moves the material from the front to the back.[2]

The working principle of friction stir processing (FSP) is based on FSW. Work is done on a single work piece instead of joining two pieces together (Figure 1). Friction stir processing technique was first reported by Mishra et al.[3] for localized microstructure modification to achieve certain desirable properties and has attracted much attention eversince.

For friction stir processing, the constituent phase material in the process zone is being mixed and refined by the tool due to the intense plastic deformation during the FSP. The true strain during FSP is approximately 40.[4] Mishra et al.[3] studied FSP with the addition of SiC and observed an increase in surface hardness as well as uniform distribution of SiC particles in Al matrix. An investigation on the effect of rotation speed on FSPed AZ31–Al_2O_3 composites, found that an increase in rotation speed led to enhancement in the particle distribution and created finer nanoparticle agglomeration.[5]

Metal matrix composites

High elastic modulus and wear resistance of particulate-reinforced metal matrix composites (MMCs) have drawn the attention of the aerospace, automobile and defence industries. Furthermore, additions of small amount of nano-sized particles significantly enhanced the material properties.[6–8]

Guo et al.[9] studied the evolution of grain structure and mechanical properties of AA6061 alloy reinforced with nano-Al_2O_3. Slurry of nano-sized Al_2O_3 particles and a volatile solvent was used to preplace reinforcing particles in an array of cylindrical holes on the surface of AA6061 plate. Multiple FSP passes were applied to improve the dispersion of the particles. In the study, particle dispersion improved with increasing number

[1]School of Mechanical & Aerospace Engineering, Nanyang Technological University, Singapore
[2]Singapore Institute of Manufacturing Technology (SIMTech), Singapore

Corresponding author:
Ming-Jen Tan, School of Mechanical & Aerospace Engineering, Nanyang Technological University, 50 Nanyang Avenue, Singapore 639798.
Email: mmjtan@ntu.edu.sg

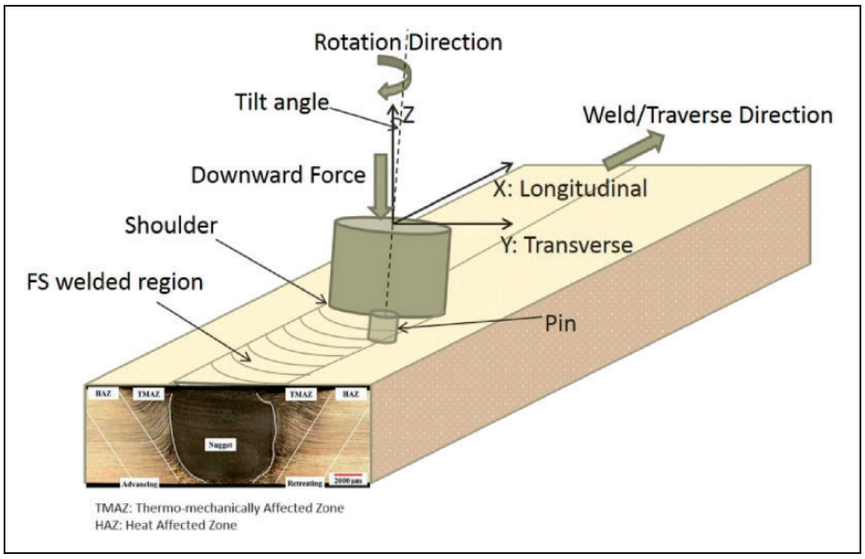

Figure 1. Schematic and actual illustration of FSP.

of FSP passes, and finer grain size was produced with the addition of composite. Also, the final grain size for one pass and three passes were similar, as the final grain size is dependent on welding temperature.[10] Liu et al.[11] studied FSP of Mg–Li–Al–Zn under water and reported fine equiaxed, recrystallized alpha (hcp), and beta (bcc) grains. Superplasticity with ductility of 300% at 100 °C and more than 400% under high strain rate at 225–300 °C was achieved.

To the best of the author's knowledge, no one has reported on CNTs reinforcement using friction stir processing. However, a study by Liao and Tan[12] was conducted on the addition of CNT to aluminum matrix. CNTs were mixed with aluminum powder and sintered before hot extrusion and hot rolling. The specimens were then tested for mechanical properties. It was observed that the presence of CNTs in the aluminum matrix slowed fatigue crack propagation by crack-bridging, CNT frictional pull-out, and breakage mechanism. Al–CNT composites showed significantly improved densification, nano-indentation modulus, hardness, tensile strength, and fatigue resistance. However, the CNTs were not well dispersed and agglomerated in clusters. FSP is able to achieve a uniform dispersion of many particles, hence the aim of this study is to use FSP to obtain uniform dispersion of the CNTs in the aluminum matrix and study its microstructure and properties.

Experimental details

There are various methods of applying particles on the substrate before performing FSP. Mishra et al.[3] prepared Al–SiC surface composites by applying a mixture of SiC powder suspended in methanol onto rolled 5083 aluminum Alloy surface. Holes, or grooves can also be made on the surface of the base material to contain the reinforcement particles.[13] Billets made from cold compacting and sintering a mixture of metal powder and composites can also be done prior to FSP.[14] Cross rolling is then done on the cast alloys to obtain a flat surface for FSP.[15]

In this study, CNTs were applied onto an AA6061-T6 rolled plate of 300 mm length and 100 mm width (rolling direction). An array of 960 cylindrical holes with diameter of 1 mm and depth of 2 mm were machined in an area of 240 mm × 50 mm (Figure 2). Acetone was used to degrease the plates before air drying. The multi-walled carbon nanotubes (MWCNTs) are of outer diameter ranging from 10 to 20 nm, length ranging from 10 to 30 μm, and purity of at least 95%. The nominal volume fraction of CNTs produced by FSP is 0.5%. A friction stir welding robot capable of generating a maximum downward force of 12 kN was used to carry out FSP. The tool used to conduct FSP was a threaded conical probe welding tool with three flats. The tool has a shoulder diameter of 12.5 mm, probe length of 2 mm, and a probe base diameter of 5 mm. An additional 1 mm thin sheet of AA6061-T6 was placed above it prior to performing FSP, using a rotational speed of 1800 r/min, travel speed of 8 mm/s, and tilt angle of 3°.

Metallographic samples were then sectioned transversely from the plates after FSP was performed. They are then polished using conventional mechanical polishing method and viewed under field emission scanning electron microscope (FESEM) equipped with electron backscattered diffraction (EBSD). EBSD was performed with step size of 0.5 μm and maps were used to plot misorientation angle histograms using Channel 5 software by HKL Technology. A minimum of five points were sampled from the cross section surface using Vickers hardness with 50 gf loading. Tensile testing was conducted in

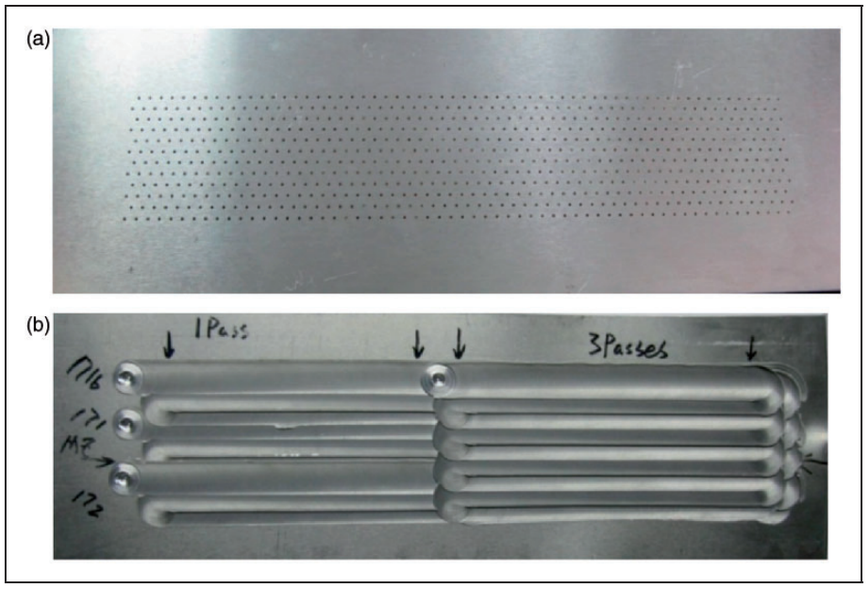

Figure 2. (a) AA6061-T6 plate with an array of 720 holes with 1 mm diameter, 1 mm in depth, and spacing of 4.2 mm; (b) AA6061-T6 plate after FSP.

accordance to ASTM E08-04 standards at test speed of 1 mm/min. A minimum of three "I"-shaped rectangular sub-sized samples with gage length of 25 mm and width of 6 mm in the reduced section were used (Figure 3). A fractography was done using scanning electron microscope (SEM) on the fractured sites.

Results and discussions

Particle dispersion

Large dendrites as well as Si particles were observed in the as-received AA6061-T6 (Figure 4(a)). FSP has broken up some Si particles and aluminum dendrites and dispersed them uniformly into the aluminum matrix. Finer particles as well as a more uniform distribution of the particles were observed with increased number of passes (Figure 4(b) and (c)). The stirred zones of the FSP were free of porosities.

Similar observations were seen in the Al–CNT SEM images. From SEM, clusters of CNTs were found in the sample with one pass (Figure 4(d)). In the sample with additions of CNT and three passes condition, there were no visible CNT clusters observed (Figure 4(d) and (e)). It is believed that the CNTs were broken up by the stirring and mixing by FSP.

Grain structure evolution

The EBSD results of the friction stir processed samples showed significant grain refinement compared to the base material (Figure 5). It was also observed to have sub-grain boundaries present in several slightly elongated grains. More sub-grain boundaries were seen in the stirred zone. This is in agreement with the continuous dynamic recrystallization, which occurred with the introduction of continuous strain coupled with rapid recovery and migration of sub-grain boundaries during friction stir processing.[16–18] Hence, severe deformation was caused by the intense dislocation generation experienced by the material in the stir zone. The stored energy in the dislocation resulted in the dynamic recovery and recrystallization process.

For samples without CNT, the average grain size is 4.49 μm for samples that underwent one pass and 5.04 μm for samples that underwent three passes (Table 1). This slight variation is in agreement with a previous study that found grain sizes are similar and independent on the number of passes.[19] And, dynamic recrystallization is a strong function of the flow stress and not the temperature during deformation.[20] Hence, the grain sizes were somewhat similar here. However, studies have also showed that grain sizes of the stir zone are a function of the welding temperature.[10,19,21] In this study, the processing parameters were kept constant for the different passes, resulting in a constant flow stress and processing temperature.

For the samples with CNT, the average grain size is 2.11 μm for samples that underwent one pass and 4.67 μm for samples that underwent three passes (Table 1). Interestingly, samples with CNT that went through three passes had larger grain sizes as compared those that went through one pass. This could be due to higher temperature experienced with the increase in number of passes with the presence of CNTs. For Al-CNTs with one pass, the average grain size is smaller than those without CNT. This could only be the result of adding CNT as the processing parameters are the same; particle stimulated nucleation may occur when Al-based metal matrix

composites were friction stir processed.[22–24] However, particle stimulated nucleation did not occur as it is only possible when dislocations accumulate at the particles during deformation and CNTs are smaller than 1 μm. Therefore, it is believed that Zener pining effect by CNT has resulted in finer grain sizes by retarding the grain growth of the matrix. The rate of grain growth in the recrystallization of metals with dispersed second phase particles can be described using equation (1) according to Humphreys et al[20]

$$\frac{dR}{dt} = M(P - P_z) = M\left(\frac{\alpha\gamma_b}{R} - \frac{3F_V\gamma_b}{2r}\right) \quad (1)$$

Here, F_v is the volume fraction, M is the boundary mobility, P is the driving pressure from the curvature of the grain boundaries, P_z is the Zener pinning pressure, R is the radius of the grain, r is the radius of the pinning particles, α is a small geometric constant, and γ_b is the boundary energy.

When $P = P_z$, grain growth will stop

$$\frac{\alpha\gamma_b}{R} = \frac{3F_V\gamma_b}{2r} \quad (2)$$

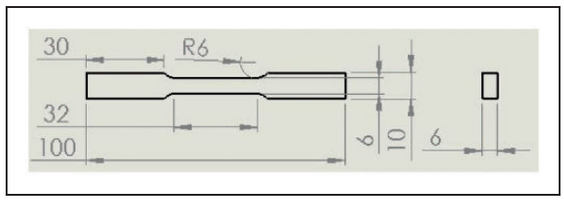

Figure 3. Dimensions of the samples used for tensile test in millimeters.

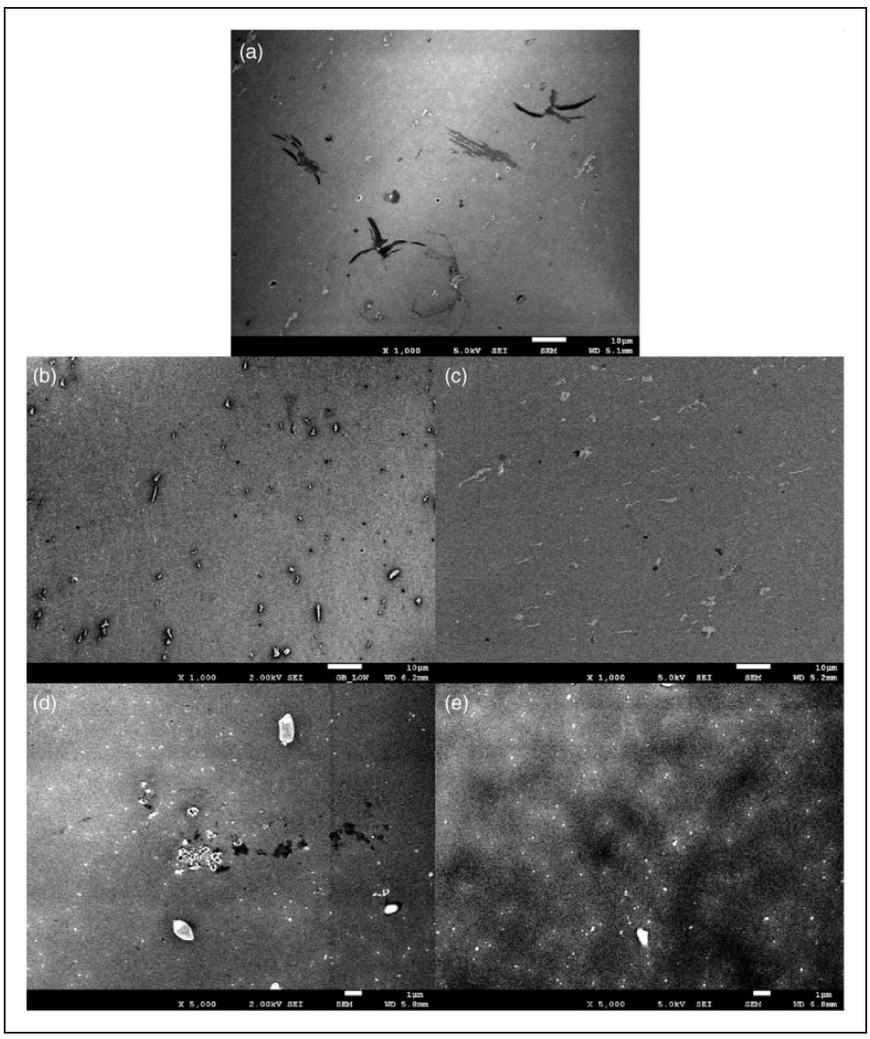

Figure 4. FESEM image of AA6061-T6 samples (a) as received with ×1000 magnification; (b) with one pass condition with ×1000 magnification; and (c) three passes with ×1000 magnification; FSP Al–CNT composite with (d) one pass with ×5000 magnification and (e) three passes with ×5000 magnification.

Zener limiting grain size ($a = 1$) can be obtained when the mean grain radius (D) and the radius of curvature (R) are taken to be the same

$$D_z = \frac{4r}{3F_v} \tag{3}$$

Tweed et al.[25] suggested that the interaction between the pinning particles and grain boundaries is very complicated. Their study suggested that the high energy of the grain boundary of the high-angle boundaries may have curved the boundary plane when it touches a second phase inclusion. This result in a bypass long before the boundary bent into a semi-circle as a whole. However, low angle boundaries has lower energy and are more flexible resulted in a more perturbed plane.

EBSD analysis was used to further investigate the pinning effect of the CNTs (Figure 6).

For friction stir processing of Al–CNT with three passes, the mean boundary misorientation and the number of high angle boundaries (>15°) was observed to have slightly decreased with a slight increase in the number of low angle boundaries (⩽15°) when compared to AA6061-T6 that underwent three passes (Table 2). The reason for this observation is that the CNTs were randomly oriented and very small in size. Hence, there were no significant pinning effect and differences in the results.

Micro-hardness

The Vickers' micro-hardness values were measured on the base material, samples without CNT, and

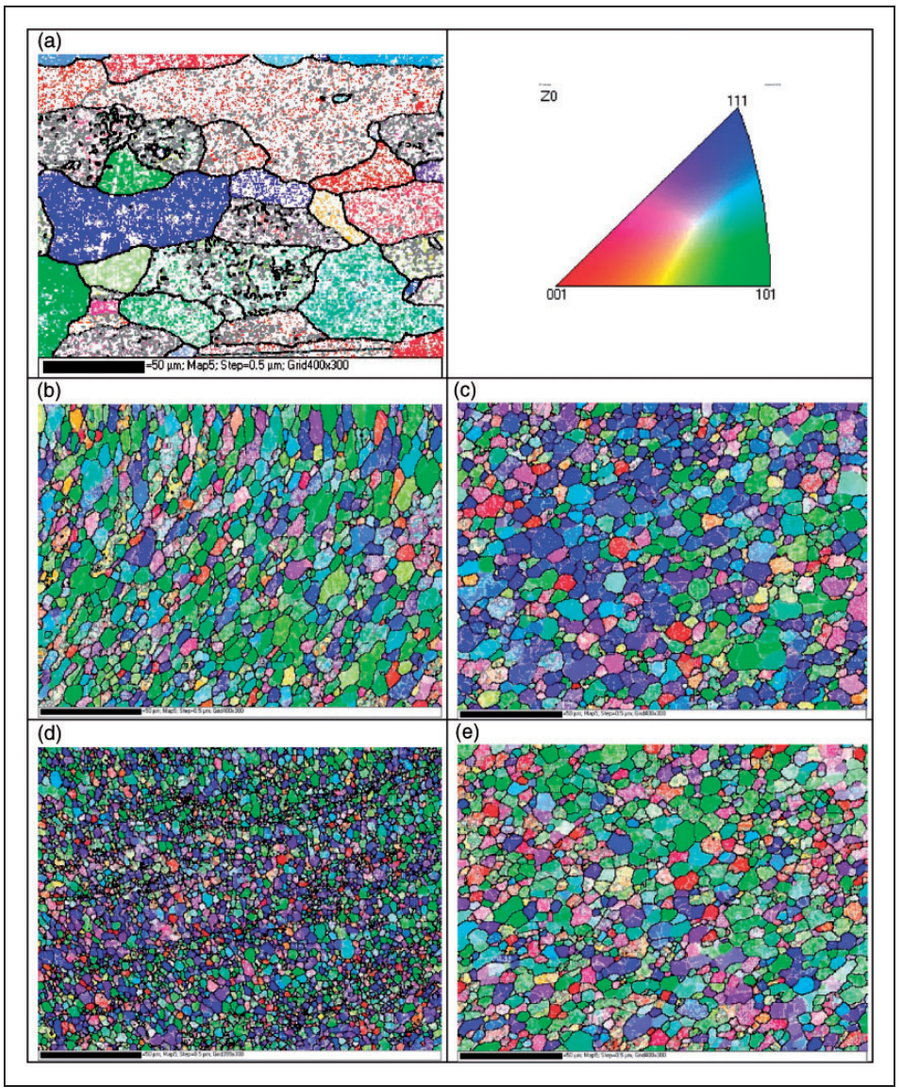

Figure 5. Typical grain structures of EBSD image of AA6061-T6 samples (a) as received, (b) with one pass condition and (c) three passes; FSP Al–CNT composite with (d) one pass and (e) three passes. For the boundary misorientation: white lines: between 1° and 5°, grey lines: between 5° and 15°, black lines: >15°. (The reader is referred to the web version of the article for interpretation of the references to colour in this figure legend.)

Table 1. Grain size measurements using EBSD.

Material and process	AA6061-T6	AA6061-T6 1 Pass	AA6061-T6 3 Passes	Al-CNT 1 Pass	Al-CNT 3 Passes
Average grain size (μm)	70.04	4.49	5.04	2.11	4.67
Standard deviation, SD	39.04	3.37	3.53	1.45	3.16

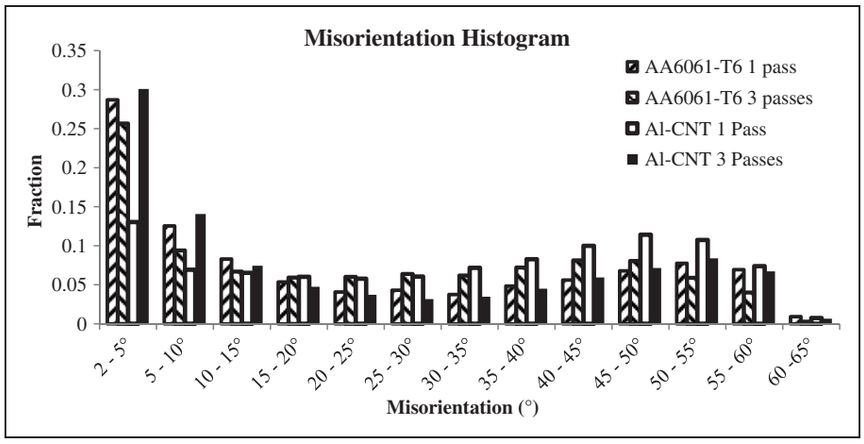

Figure 6. Histogram showing the distribution of grain/sub-grain misorientation angle by EBSD.

Table 2. Grain/ sub-grain boundary misorientations.

Material and process	Mean grain misorientation (°)	Fraction of high-angle grain boundaries (>15°)	Fraction of low angle grain boundaries (⩽15°)		Number of samples
			(1–5°)	(0–15°)	
AA6061-T6 1 Pass	23.11	0.50	0.29	0.50	49,871
AA6061-T6 3 Passes	24.00	0.58	0.26	0.42	39,629
Al-CNT 1 Pass	31.14	0.74	0.13	0.26	71,873
Al-CNT 3 Passes	22.75	0.48	0.30	0.52	50,795

Table 3. Micro-hardness values measurement of the base material, FSP of base material and FSP of Al–CNT composite.

Materials and process	AA6061-T6	AA6061-T6 1 Pass	AA6061-T6 3 Passes	Al–CNT 1 Pass	Al–CNT 3 Passes
HV	109.5	61.7	66.2	80.1	90.6
Standard deviation	1.38	1.70	0.72	0.93	0.87

samples with CNTs added (Table 3). The decrease in hardness value was observed when FSP was conducted on AA6061-T6. It is also observed that increasing the number of passes did not influence the hardness of the samples without CNT. This could be due to the dissolution of the hardening precipitates.[26]

For Al–CNT composites, significant improvement in the hardness value was observed when comparing with those friction stir processed samples without CNTs. This is due to the finer grain sizes and the Orowan strengthening caused by the addition of CNTs. An increase in the hardness value was observed with the increase in the number of passes. This could be due to the improved dispersion of the CNTs under three pass conditions.

Tensile testing

The tensile stress strain verses strain curves were plotted as shown in Figure 7. The tensile results of FSP samples without CNTs showed that a decrease in yield strength compared to a non-FSP sample (Table 4). There is also a significant increase in percentage elongation-to-failure, indicating an improvement in ductility. This is mainly due to the grain

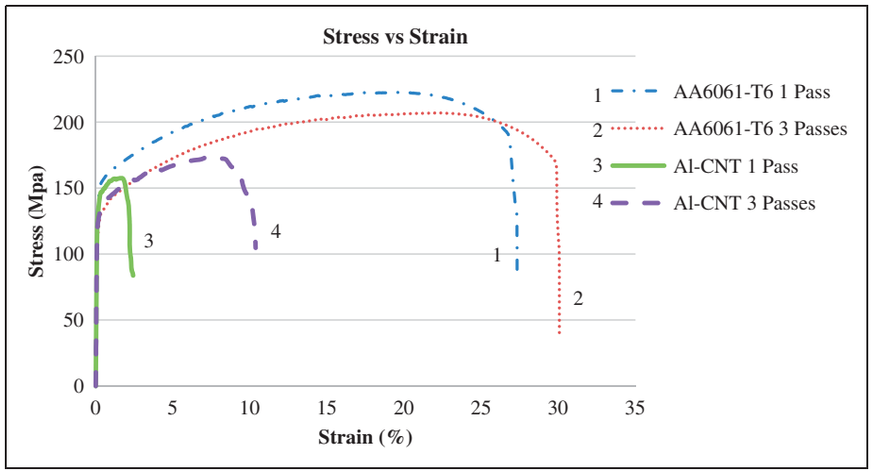

Figure 7. Stress versus strain plot of friction stir processed samples.

Table 4. Tensile results.

Tensile properties of Al base metal and Al–CNT composites produced by FSP

Materials and process	Ultimate tensile strength (MPa)	Yield strength (MPa)	Elongation (%)	Young's modulus (GPa)
AA6061-T6[27]	290	240	8	69
AA6061-T6 1 Pass	220 ± 4	110 ± 4	27 ± 1	71 ± 1
AA6061-T6 3 Passes	206 ± 2	96 ± 9	29 ± 1	71 ± 1
Al–CNT 1 Pass	157 ± 4	120 ± 5	3 ± 1	57 ± 2
Al–CNT 3 Passes	178 ± 28	112 ± 2	10 ± 5	65 ± 12

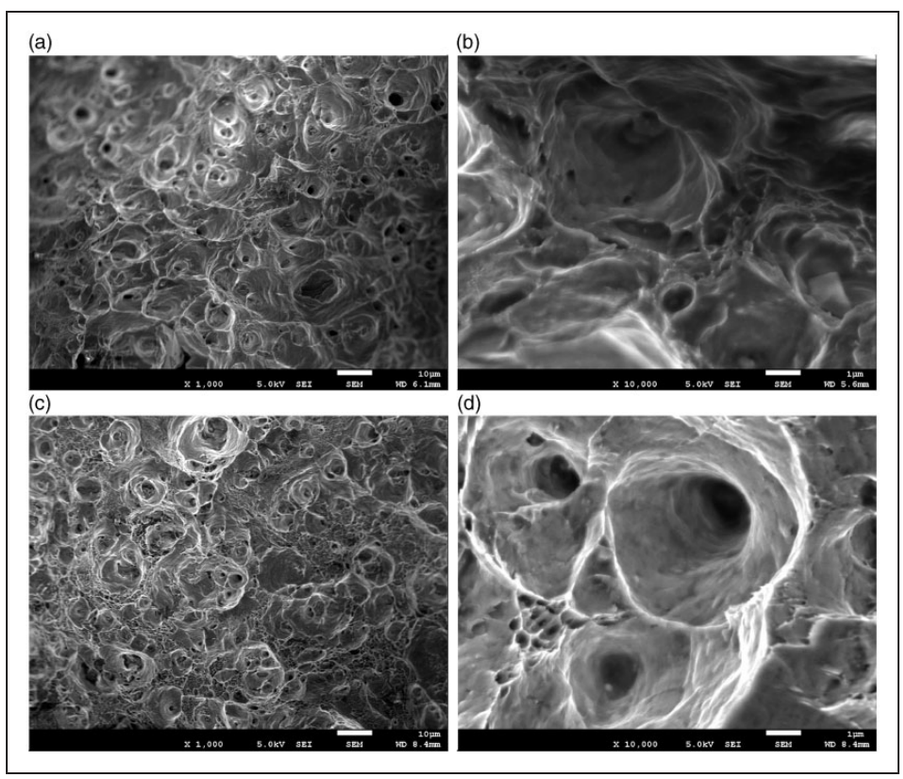

Figure 8. SEM image of the fracture site of the FSP monolithic Al plates with (a) one pass condition with ×1000 magnification; (b) one pass with ×10,000 magnification; (c) three passes with ×1000 magnification; and (d) three passes with ×10,000 magnification.

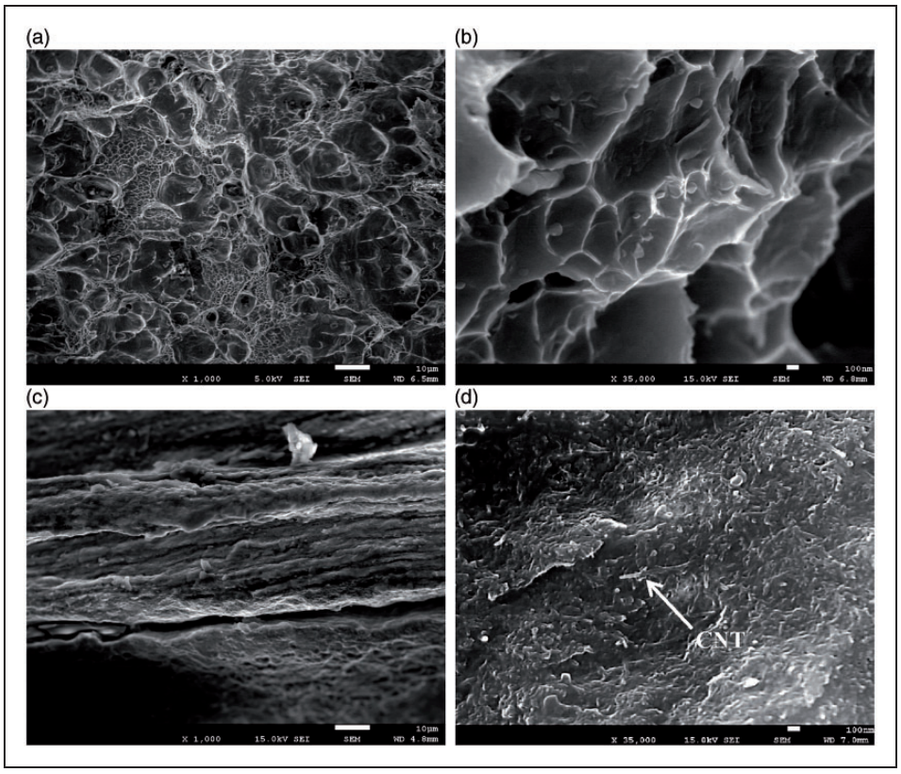

Figure 9. SEM image of the fracture site of the FSPed Al–CNT samples: (a) one pass condition under ×1000; (b) one pass under ×10,000; (c) three passes under ×1000; (d) three passes under ×10,000.

refinement (Figure 4). A reduction in the yield strength was observed when comparing one pass and three passes; this could be due to the dissolution of the hardening precipitates.[26]

The tensile results from the FSP with CNTs showed no improvement in yield strength as compared to the parent material (AA6061-T6) without FSP (Table 4). However, the yield strength of Al–CNT was superior when compared to FSP without any addition of CNTs. For Al–CNT samples, there was a significant reduction in the percentage elongation-to-failure in both one and three passes. The CNTs could have acted as defects and stress concentrators during the tensile test. The strengthening of the material could be attributed to the grain size differences from Hall–Petch equation.[9]

Fractography

The fracture sites of the FSP samples without CNTs were observed under SEM and dimpled appearances at the fracture sites were observed indicating ductile fracture. In addition, smaller dimples were observed in FSP samples that underwent three passes (Figure 8).

For the FSP samples with CNTs, larger dimples were found on the samples with one pass condition compared to three passes. This is in agreement with the tensile results earlier indicating three passes is more ductile than one pass. Some CNTs were observed in the SEM (Figure 9).

Comparing the percentage elongation-to-failure of the specimens with and without CNT, the specimen with CNT had smaller percentage elongation-to-failure. This observation implies that specimens with CNT are less ductile. In addition, some CNTs were observed at the fracture site, indicating the CNTs could have acted as defects in the material under tensile load. The interaction between the CNTs and the Al matrix may not be strong enough in enhancing of the mechanical properties. The appearance of CNTs at the fracture sites of the samples that underwent three passes also suggested that crack bridging could have occurred.[12,28]

Conclusion

1. In this work, FSP on monolithic AA 6061 plates and Al–CNT composites were studied together with the effects of different number of passes. For the monolithic Al 6061, the dendrites were broken down and dispersed uniformly with the increase in the number of passes. In the study of FSP of Al-CNT composite, the CNTs have been successfully dispersed with three FSP passes; dispersion is more uniform with the increasing number of passes.

2. The Vickers hardness number decreased with increasing number of passes for the AA6061 specimens that underwent FSP due to dissolution of the hardening precipitates. For specimens with CNTs, the Vickers hardness increased with increased number of passes. Overall, the specimens with CNT have superior hardness values than specimens without CNT that underwent FSP, but inferior to the as-received AA6061-T6 specimens.
3. Grain refinement was achieved using FSP. The addition of CNT resulted in further refinement of the grains, improved tensile yield strength as well as provided crack bridging in the material. The ductility of the material improved with increased number of passes.

Conflict of interest

None declared.

Funding

This research received no specific grant from any funding agency in the public, commercial, or not-for-profit sectors.

References

1. Thomas WM, Nicholas ED, Needham JC, et al. In: 9125978.8 GBPAN (ed.), December 1991.
2. Reynolds AP. Visualisation of material flow in autogenous friction stir welds. *Sci Technol Weld Join* 2000; 5: 120–124.
3. Mishra RS, Ma ZY and Charit I. Friction stir processing: A novel technique for fabrication of surface composite. *Mater Sci Eng A* 2003; 341: 307–310.
4. Heurtier P, Desrayaud C and Montheillet F. *A thermomechanical analysis of the friction stir welding process*. Materials Science Forum. Switzerland: Trans Tech Publications, 2002, pp.1537–1542.
5. Azizieh M, Kokabi AH and Abachi P. Effect of rotational speed and probe profile on microstructure and hardness of AZ31/Al2O3 nanocomposites fabricated by friction stir processing. *Mater Des* 2011; 32: 2034–2041.
6. Miracle DB. Metal matrix composites – From science to technological significance. *Compos Sci Technol* 2005; 65: 2526–2540.
7. Guo J, Gougeon P and Chen XG. Study on laser welding of AA1100-16 vol.% B4C metal–matrix composites. *Compos Part B: Eng* 2012; 43: 2400–2408.
8. Chawla N and Chawla KK. *Metal matrix composites*. New York: Springer, 2006.
9. Guo JF, Liu J, Sun CN, et al. Effects of nano-Al2O3 particle addition on grain structure evolution and mechanical behaviour of friction-stir-processed Al. *Mater Sci Eng A* 2014; 602: 143–149.
10. Sato Y, Urata M and Kokawa H. Parameters controlling microstructure and hardness during friction-stir welding of precipitation-hardenable aluminum alloy 6063. *Metall Mater Trans A* 2002; 33: 625–635.
11. Liu FC, Tan MJ, Liao J, et al. Microstructural evolution and superplastic behavior in friction stir processed Mg–Li–Al–Zn alloy. *J Mater Sci* 2013; 48: 8539–8546.
12. Liao JZ and Tan MJ. Improved tensile strength of carbon nanotube reinforced aluminum composites processed by powder metallurgy. *Adv Mater Res* 2012; 500: 651–656.
13. Qu J, Xu H, Feng Z, et al. Improving the tribological characteristics of aluminum 6061 alloy by surface compositing with sub-micro-size ceramic particles via friction stir processing. *Wear* 2011; 271: 1940–1945.
14. Zahmatkesh B and Enayati MH. A novel approach for development of surface nanocomposite by friction stir processing. *Mater Sci Eng A* 2010; 527: 6734–6740.
15. Liu FC, Ma ZY and Zhang FC. High strain rate superplasticity in a micro-grained Al–Mg–Sc alloy with predominant high angle grain boundaries. *J Mater Sci Technol* 2012; 28: 1025–1030.
16. Su J-Q, Nelson TW and Sterling CJ. Microstructure evolution during FSW/FSP of high strength aluminum alloys. *Mater Sci Eng A* 2005; 405: 277–286.
17. Guo J, Amira S, Gougeon P, et al. Effect of the surface preparation techniques on the EBSD analysis of a friction stir welded AA1100-B4C metal matrix composite. *Mater Charact* 2011; 62: 865–877.
18. Fonda RW, Knipling KE and Bingert JF. Microstructural evolution ahead of the tool in aluminum friction stir welds. *Scripta Mater* 2008; 58: 343–348.
19. Brown R, Tang W and Reynolds AP. Multi-pass friction stir welding in alloy 7050-T7451: Effects on weld response variables and on weld properties. *Mater Sci Eng A* 2009; 513–514: 115–121.
20. Humphreys FJ and Hatherly M. Hot deformation and dynamic restoration. In: FJ Humphreys and M Hatherly (eds) *Recrystallization and related annealing phenomena*. 2nd ed. Oxford: Elsevier, 2004, pp.415–450.
21. Hassan KAA, Norman AF, Price DA, et al. Stability of nugget zone grain structures in high strength Al-alloy friction stir welds during solution treatment. *Acta Mater* 2003; 51: 1923–1936.
22. Guo J, Gougeon P and Chen XG. Microstructure evolution and mechanical properties of dissimilar friction stir welded joints between AA1100-B4C MMC and AA6063 alloy. *Mater Sci Eng A* 2012; 553: 149–156.
23. Shahani RA and Clyne TW. Recrystallization in fibrous and particulate metal matrix composites. *Mater Sci Eng A* 1991; 135: 281–285.
24. Root JM, Field DP and Nelson TW. Crystallographic texture in the friction-stir-welded metal matrix composite Al6061 with 10 Vol Pct Al2O3. *Metall Mater Trans A* 2009; 40: 2109–2114.
25. Tweed CJ, Ralph B and Hansen N. The pinning by particles of low and high angle grain boundaries during grain growth. *Acta Metall* 1984; 32: 1407–1414.
26. Al-Fadhalah KJ, Almazrouee AI and Aloraier AS. Microstructure and mechanical properties of multi-pass friction stir processed aluminum alloy 6063. *Mater Des* 2014; 53: 550–560.
27. *ASM handbook / prepared under the direction of the ASM International Handbook Committee*. Materials Park, OH: ASM International, 1986.
28. Liao JZ, Tan MJ and Santoso A. High strength aluminum nanocomposites reinforced with multi-walled carbon nanotubes. *Adv Mater Res* 2011; 311–313: 80–83.